# Numerical analysis of the stress-strain state of the steel superficial layer under nanostructuring burnishing

Igor Yu. Smolin Viktor P. Kuznetsov Andrey I. Dmitriev
smolin@ispms.tsc.ru

**Abstract**

In this paper the theoretical study of the problem of stress-strain state of the surface of the steel at burnishing is performed within the framework of computer simulation. A dynamic formulation of the problem which allows more accurate description of the process details is used. The finite element method in the approximation of plane strain condition is used. The burnishing tool or indenter was modeled by an absolutely rigid body, and for steel the model of elastic-plastic body with isotropic hardening according to the experimentally defined law was adopted. The patterns of stress-strain state of the material near the treated surface and the mechanisms of nanostructure formation in the surface layer were analyzed. The influence of the parameters of the burnishing process as burnishing force and friction coefficient on the features of stress and plastic strain distribution formed is investigated. The simulation results are compared with experimental data.

## 1 Introduction

Surface burnishing on modern multiprocessing machines is a highly efficient method of surface finish of high-precision parts [1, 2, 3]. A considerable increase in hardness, wear resistance, and fatigue strength of structural steel surfaces can be attained by nanostructuring burnishing in which indenters with increased friction coefficients and thermal stability ensure a high shear strain level [2]. Nanostructuring burnishing forms an enlarged bulge of plastically edged metal which is a stress microconcentrator assisting structural dispersion of a thin surface layer. However, the growth of the bulge can lead to destabilization of the dynamic burnishing system and initiate self-vibration [3]. Thus, nanostructuring surface burnishing of structural steels requires theoretical substantiation of its modes to control plastic strain accumulation without impairing the dynamic stability of the process. Another important problem is to clarify the effect of the ratio between the burnishing force and the friction coefficient of the indenter material on the character of deformation processes.

Note that the existing theoretical models [4] based on analytical description and the numerical models that use static problem statements fail to reproduce in full measure the actual pattern of the processes occurring in a thin superficial layer in burnishing, the more so in nanostructuring burnishing. This is due to both dynamics of the process and extremely complex non-uniform stress-strain distribution in the thus loaded material. A more preferable way is to use numerical simulation methods in which the set of differential equations of solid mechanics is integrated with regard for boundary conditions and elastoplastic properties of a surface layer of test material.

Thus, the objective of the work was to study the process of nanostructuring burnishing and the peculiarities of the stress-strain state of a superficial layer of the treated material by the dynamic variant of the finite element method and with a specified constant indenter pressing force, but not depth. Those two compose is the main difference of our approach from conventional ones used to study the stress-strain state of a near-surface layer under burnishing or friction treatment. The primary task was to determine the peculiarities of the stress-strain state capable of providing the mechanisms of the nanostructured surface layer formation –вЂ“ friction-induced shear and rotational deformation.

## 2 The numerical model description

We simulated burnishing of a steel specimen in the two-dimensional statement for the plane stress state. The calculations were performed by the ANSYS/LS-DYNA finite element program. We chose a mesh of four-node quadrilateral elements with linear interpolation of the quantities. The mesh had increasing density from the bottom upwards to provide sufficient details of the mesh near the contact surface. The surface loading was specified through calculating the interaction between the upper face of the deformed specimen and the indenter which was an absolutely rigid body with its boundary being part of a cylinder of radius $R = 2\ mm$. The process simulation was realized in two stages. First, the indenter was pressed into the specimen with a constant force $P$, whereupon it moved under this force with a constant velocity $V = 10$ m/min. A scheme of the model specimen and loading conditions is shown in Fig.1. At the top of the rectangle, a part of the indenter is depicted with indication of the burnishing force $P$ and indenter velocity $V$. The rectangle framed on three sides corresponds to a part of the treated specimen with boundary conditions of вЂ“slidingвЂќ or symmetry (displacements perpendicular to the boundaries are prohibited). The dimensions of the calculation domain were $4792\times1995\ \mu m$.

The parameters varied in the investigation were the friction coefficient $\mu$ and the burnishing force $P$. In one calculation, the sliding friction coefficient $\mu$ and the burnishing force $P$ were fixed. The initial specimen surface was taken to be perfectly smooth.

The mechanical characteristics of the specimen were taken to correspond to steel 20X (Russian designation): YoungвЂ™s modulus $E = 218$ GPa, PoissonвЂ™s ratio $\nu = 0.267$, and density $\rho = 7670\ kg/m^3$. The mechanical behavior was described by an elastoplastic model with the von Mises yield criterion and isotropic hardening. Because the real process involves cooling of the specimen surface and indenter, the heat produced in friction and its effect on the strength characteristics of the steel were ignored.

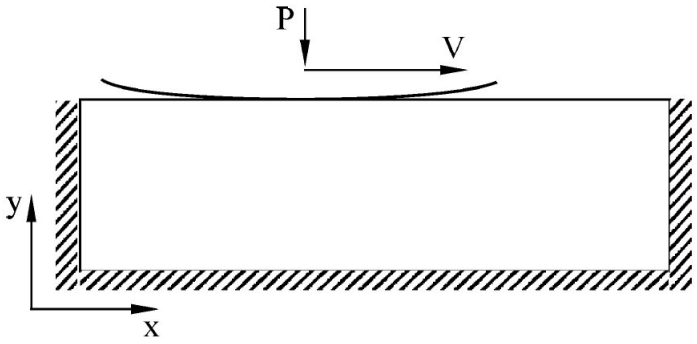


Figure 1: Schematic diagram of the model specimen and loading conditions.

The hardening curve was determined by special experiments [5]. The strain hardening diagram obtained is presented in Fig.2.

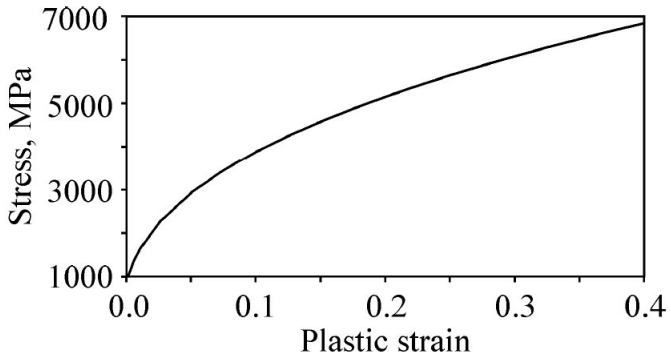


Figure 2: Strain hardening curve $\sigma_s(\varepsilon_{eq}^{pl})$.

# 3 Results of modeling

## 3.1 Plastic strain accumulation during burnishing

Figure 3 shows a chronogram of the effective accumulated plastic strain distributions in the specimen loaded by a moving indenter. It is seen that ahead of the moving indenter, a bulge of edged material was formed. The plastic strains in the bulge are small, but the vertical displacements are maximal. It can also be traced on the chronogram that a part of the material near the surface is entrained by the indenter; therefore, the position of points 2 and 3 by the end point in time is close to the right boundary of the cutout spatial domain.

Analysis of variations in accumulated plastic strains shows that under dynamic loading, high plastic strains are generated and accumulated beneath the moving indenter. So in a narrow near-surface layer of thickness 75 $\mu m$, they reach $\sim 100\%$ and decrease in going deep into the material; at a depth of $\sim 500$ $\mu m$, the plastic strains are $\sim 10\%$.

In multiple passes of the indenter, plastic strain accumulation depends strongly on the form a hardening curve. If the hardening curve tends to a certain limiting value (to saturation), the strains increase non-uniformly. If the hardening curve is approximated by a power function as in Fig.2, considerable plastic strains are accumulated in the first pass and they remain further almost unchanged. This means that a large number of passes can be inefficient for hardening the material and providing its other functional properties. As one would expect, increasing the friction coefficient and the burnishing force increases the accumulated plastic strains in the thin surface layer subjected to nanostructuring burnishing [2].

## 3.2 Effect of the friction coefficient and the burnishing force on the height of a bulge of edged material

The impact of the friction coefficient and the burnishing force on the height of the edged material bulge was analyzed from the diagrams of vertical displacements of the same point (No. 5) of the treated surface. The bulge height was determined as a difference of the maximum lift in the bulge and the deepest sink for the point before arrival of the indenter.

The effect of both burnishing parameters on the formation of the edged material bulge is represented in Fig.4. It is seen that the increase in the height of the edged material bulge with increasing the friction coefficient and the burnishing force obeys a nonlinear increasing dependence. Analysis of the calculation data also suggests that if the burnishing force is small, the bulge is hardly formed at all at friction coefficients of up to 0.35. Additional

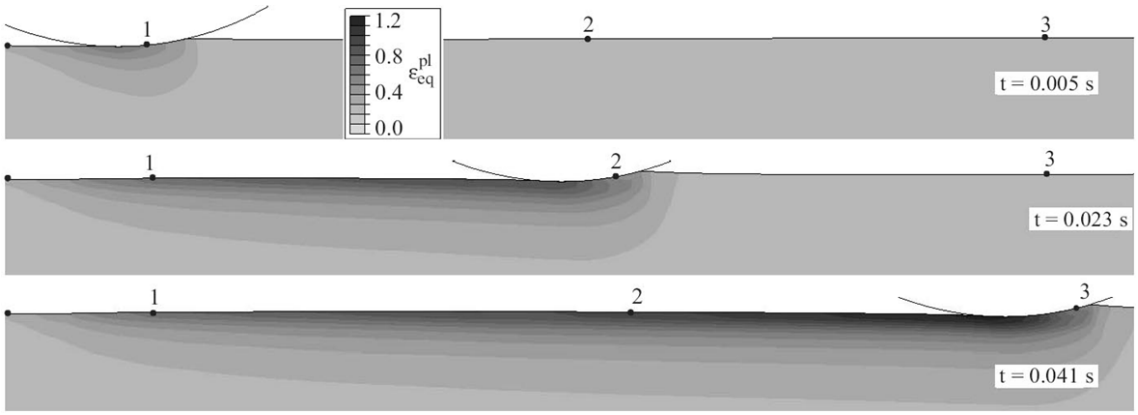


Figure 3: Chronogram of the distribution of equivalent accumulated plastic strains. The layer thickness is 580 $\mu m$.

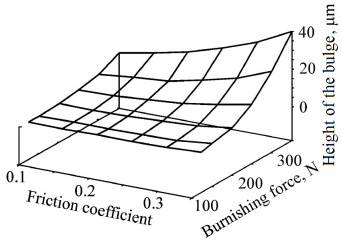


Figure 4: Height of the bulge versus the friction coefficient and the burnishing force.

calculations show that only at a very high friction coefficient ($\mu = 0.5$), the material is edged a little.

### 3.3 Stress distribution at the deformation site

Because the edged material bulge grows with an increase in both burnishing force and friction coefficient, let us analyze the stress distribution first for the case when the parameters are both high (the friction coefficient is 0.35 and the burnishing force is 350 N.

Figure 5a shows the indenter position, the deformed finite element mesh, and the two-dimensional distribution of shear stresses $\sigma_{xy}$ in the computational domain. Figure 5b and 5c show diagrams of the stress tensor components $\sigma_{xx}$, $\sigma_{yy}$ and $\sigma_{xy}$ and also the pressure $P_s$ and the equivalent stresses $\sigma_{eq}$ along two lines indicated by markers in Fig.5a. The abscissa is the distance from the edge of the marked line along the $x$ axis.

By and large, joint analysis of all stress components suggests that in the layers nearest to the surface, the stress state upstream of the deformation site is similar to axial compression and that downstream of this site it is similar to uniaxial tension. At the deformation site, a complex stress state takes place.

In a deeper material layer, a different stress state downstream of the indenter is realized. It is seen that the lower line of markers in Fig.5a crosses not only the region of positive shear stresses at the right (a wedge) but also the region of negative shear stresses at the left beneath the indenter.

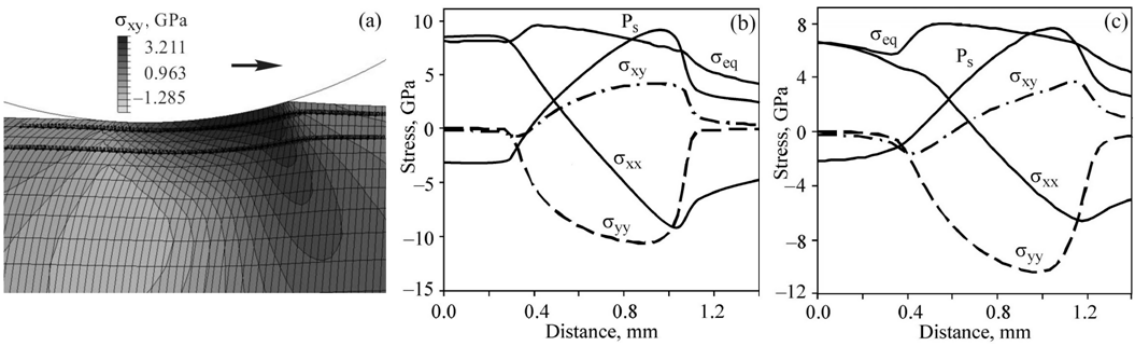


Figure 5: Distribution of shear stresses at the deformation site (a) and different stress components along two lines at the surface (indicated by markers in (a)): b — for the upper line, c — for the lower line with a large bulge of edged material. The direction of indenter motion is indicated by an arrow.

The foregoing character of the stress distribution can explain the rotation-shear deformation in a surface layer, because the indenter motion causes the uppermost surface region to experience alternate loads close to axial compression-tension and those deeper from the surface to experience alternate shear. In the upper surface layers, the plastic strains are thus higher than the plastic strain in the deeper material layers.

Another conclusion from the analysis of the stress distributions is that fracture of the surface layer is possible at high friction coefficients, because the normal tensile stresses can exceed the ultimate strength of the material.

Let us now consider the stress distribution at the deformation site when the bulge is hardly formed: the burnishing force is $P = 122.5$ N and the friction coefficient is 0.07. The stress distribution in near-surface layers qualitatively fits that for a large bulge. A difference is found only in the shear stresses $\sigma_{xy}$, whose distribution is closer to a symmetric one with respect to the indenter vertex. In deeper layers, a qualitative difference is found in the normal stress distribution $\sigma_{xx}$; in this case, no transition from compression upstream of the indenter to tension downstream of it is observed. All layers experience compression. Note, that the stress distribution patterns obtained in our calculations agree qualitatively with the data of numerical experiments [4].

## 4 Discussion and concluding remarks

The most important result of the study is a disclosure of the conditions conductive to the formation of a nanostructured near-surface layer in burnishing. In particular, analysis of the numerical simulation results shows that motion of the indenter along the burnished surface gives rise to a complex stress-strain state in the material region near the indenter and its dynamics reveals an alternating character. Multiple passes of the indenter along the surface of a treated part during its rotation on a machine create cyclic alternate loads on superficial layers of the material. The available methods of severe plastic deformation resulting in nanostructured bulk metal materials are characterized by large degrees of shear strains with a variable stress-strain state [6]. The probability of these conditions to occur in frictional hardening of steels is also pointed out elsewhere [7].

The experiments [2] confirm the formation of nanostructured layers in burnishing. So, transmission electron microscopy shows that in a thin surface layer of carburized steel 20X subjected to nanostructuring burnishing by an indenter with a high friction coefficient

($\mu = 0.35$), a homogeneous ultrafine-grained structure with martensite crystallite sizes of $20 - 50$ $nm$ is formed (Fig.6b and 6c). The electron diffraction patterns in the form of continuous Debye rings suggest that individual fragments are misoriented at angles ranging to several tens of degrees. The rotational plasticity in nanostructuring surface burnishing of steel 20X ensures the formation of nanocrystalline structures in a surface layer at a depth of up to $5 - 7$ $\mu m$ (Fig.6a).

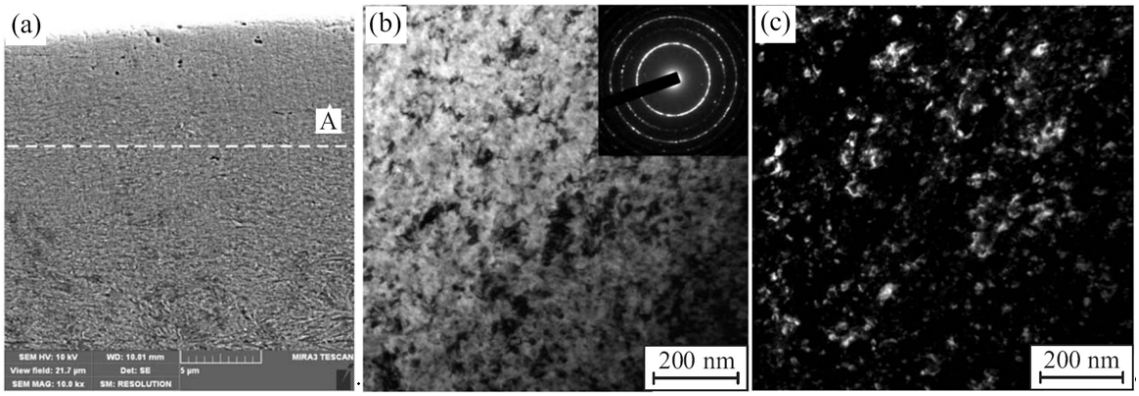


Figure 6: Scanning and transmission electron microscopy of a thin surface layer of carburized steel 20X subjected to nanostructuring burnishing by a tool with a dynamic stabilization unit on a turn-mill center: A — nanostructured layer boundary.

Thus, the distribution of accumulated plastic strains and stresses in the upper layers of the burnished surface shows that a narrow superficial layer undergoes certain peculiar severe plastic deformation. It is this action on the surface layer material that can provide the formation of a nano-grained structure in burnishing. The results of numerical simulation demonstrate that the depth of a superficial layer subjected to external action is determined by the process parameters: the burnishing force and the friction coefficient. So, increasing the friction coefficient increases the shear stresses and the accumulated plastic strains, and this assists the formation of nanostructural states. On the other hand, at very high friction coefficients, the burnishing mode can change with break of the contact and fracture of the surface layer material.

## References

[1] Korzynski, M. and Pacana, A., Centreless Burnishing and Influence of its Parameters on Machining Effects, J. Mater. Process. Tech., 2010, vol. 210, no. 9, pp. 1217–1223.

[2] Kuznetsov, V.P., Makarov, A.V., Pozdeeva, N.A., Savrai, R.A., Yurovskii, A.S., Malygina, I.Yu., and Kiryakov, A.E., Enhancement in Strength, Heat and Wear Resistance in Parts of Carburized 20X Steel by Nanostructuring Burnishing using Turn/Mill Machines, Uprochn. Tekhnol. Pokryt., 2011, no. 9, pp. 3–13.

[3] Kuznetsov, V.P., Simulation of the Effect Technological Parameters on Vibration Resistance in Surface Burnishing, Metalloobrabotka, 2010, vol. 55, no. 1, pp. 7–15.

[4] Smelyanskii, V.M., Mechanics of Material Strengthening by Surface Plastic Deformation, Moscow: Mashinostroenie, 2002.

[5] Konovalov, D.A., Smirnov, S.V., and Konovalov, A.V., Determination of Metal Strain-Hardening Curves from Conical Indenter Impression Results, Russ. J. Nondestr. Test., 2008, no. 12, pp. 55–63.

[6] Valiev, R.Z., Estrin, Yu., Horita, Z., Langdon, T.G., Zehetbauer, M.J., and Zhu, Yu.T., Producing Bulk Ultrafine-Grained Materials by Severe Plastic Deformation, JOM, 2006, vol. 4, pp. 33–39.

[7] Vichuzhanin, D.I., Makarov, A.V., Smirnov, S.V., Pozdeeva, N.A., and Malygina I.Yu., Stress-Strain State and Damage at Friction Strengthening of Steel Plane Surface by Cylindrical Indenters, Problem. Mashinoved. Nadezhn. Mashin, 2011.

*Igor Yu. Smolin, Akademichesky 2/4, 634021, Tomsk, Russia*
*Viktor P. Kuznetsov, Gogol str. 25, 640000, Kurgan, Russia*
*Andrey I. Dmitriev, Akademichesky 2/4, 634021, Tomsk, Russia*